Measurement of Single Top-Quark Production Cross Section at DØ

Yun-Tse Tsai([1]), on behalf of the DØ Collaboration
([1]) *University of Rochester - Rochester, N.Y.*

Summary. — We present a new measurement of the electroweak single top-quark production cross section in proton-antiproton (p-$\bar{p}$) collisions at $\sqrt{s} = 1.96$ TeV in 9.7 fb^{-1} of integrated luminosity collected with the DØ detector. We select signal-like events, containing one energetic electron or muon, an imbalance in transverse momentum, and two or three jets, with one or two identified as candidates for originating from the fragmentation of b quarks. A discriminant based on the "Matrix Element" method is used to separate the signal from background. The s and t-channel cross sections for producing a single top quark are expected to be $\sigma(p\bar{p} \to tb + X) = 1.05^{+0.38}_{-0.35}$ pb and $\sigma(p\bar{p} \to tqb + X) = 2.26^{+0.58}_{-0.54}$ pb. The probabilities to measure these values or larger of cross section in absence of signal are expected to be 3.3 and 4.9 standard deviation significance for the s and t-channel, respectively.

PACS 12.15.Ji – Applications of electroweak models to specific processes.
PACS 13.85.Qk – Inclusive production with identified leptons, photons, or other nonhadronic particles.
PACS 14.65.Ha – Top quarks.

1. – Introduction

Top quarks are produced as $t\bar{t}$ pairs via the strong interaction, or singly via the electroweak interaction [1,2]. At the Tevatron, single top quarks proceed mainly through the decays of an off-shell (virtual) W boson in the s-channel, accompanied with a bottom quark ("tb" final state) as shown in Fig. 1(a) [3], or through the fusion of a virtual W boson with an incident virtual b quark in the t-channel, associated with a b and a first-generation quarks ("tqb" final state) as shown in Fig. 1(b) [4, 5]. Measuring the single top-quark production cross section provides a direct determination of the magnitude of the Cabibbo-Kobayashi-Maskawa (CKM) [6] matrix element $|V_{tb}|$ [7], and an indirect measurement of the width and lifetime of the top quark [8]. In addition, physics beyond the standard model (SM) can change the cross sections of the s and t-channel differently; the s-channel is sensitive to new particles, such as charged Higgs and W' bosons [9-11], while the t-channel is affected by anomalous Wtb couplings [12, 13] and flavor-changing neutral currents (FCNC) [9,14]. Measuring the single top-quark production cross section

precisely, as well as the s and t-channels individually, can therefore help to disentangle different models of physics beyond the SM. However, owing to the small cross section and overwhelming background contamination, the measurement is difficult, and the inclusive single top-quark production was therefore observed in 2009 [15, 16], 14 years after the observation of top-quark production in pairs [17, 18].

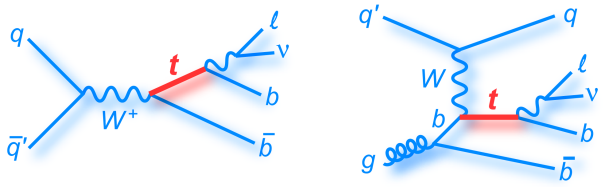

(a) (b)

Fig. 1. – Leading-order Feynman diagrams for electroweak single top-quark production for (a) s-channel "tb" mode, and (b) t-channel "tqb" mode.

In this analysis, we assume the branching ratio of the top quark to Wb is 100%, which only requires $|V_{tb}|^2 \gg |V_{td}|^2 + |V_{ts}|^2$, but does not constrain the number of elementary fermion generations (i.e. to three in the SM) nor the unitarity of the CKM matrix. To reduce multijet events produced via the strong interaction, we only consider the events that contain an isolated electron or muon in the final state in this analysis, namely, the events with leptonic W decay.

2. – Event Selection

We analyze the full Tevatron Run II data sample collected at the DØ detector, corresponding to an integrated luminosity of 9.7 fb^{-1}. We select events that contain one isolated high-p_{T} electron or muon, an imbalance in transverse momentum to account for the presence of a neutrino, and two or three jets in the final state. The electrons or muons have to satisfy the criteria of $p_{\mathrm{T}} > 20$ GeV, $|\eta| < 1.1$ for electrons and $|\eta| < 2.0$ for muons. The imbalance in transverse momentum $\not\!\!E_T$ is required to be 20 (25) $< \not\!\!E_T < 200$ GeV for events with two (three) jets. The jets have to fulfill $p_{\mathrm{T}} > 20$ GeV and $|\eta| < 2.5$, and the highest-p_{T} (leading) jet must satisfy $p_{\mathrm{T}} > 25$ GeV. By requiring a criterion on the scalar sum over the transverse momentum of all final-state objects (H_T), $H_T > 120$ (140) GeV for events with two (three) jets, the multijet backgrounds are greatly reduced. To further enhance the signal purity, one or two of the jets are required to be identified as candidates for originating from the fragmentation of b quarks (b-tagging).

We use Monte Carlo (MC) simulation to model the signal and background. The CompHEP-based SINGLETOP event generator [19] is exploited for the single top-quark signal, where the kinematics of the generated events match to the next-to-leading order (NLO) prediction, providing effectively the NLO event kinematics. The ALPGEN leading-log MC event generator [20] is used to model the $t\bar{t}$, W+jets, and Z+jets backgrounds, while the WW, WZ, and ZZ diboson events are simulated using PYTHIA [21]. These event generators are interfaced to PYTHIA for the modeling of hadronization. All generated MC events are processed through the GEANT simulation [22] of the DØ detector to model the detector and reconstruction effects. The details of the DØ detector and recon-

struction algorithm can be found in Ref. [23]. Several correction scale factors are applied in the simulated samples to account for differences between reconstruction efficiencies in simulation and data.

The multijet background is modeled using data events that contain a none-isolated electron or muon, and, the contributions of those events, as well as of the W+jets events, are scaled to data simultaneously in the sample without the b-tagging criteria, where the signal contribution is less then 1%.

A b-tagging algorithm based on a multivariate technique is used to identify jets as originating from the fragmentation of b quarks (b jets) [24]. Two non-overlapping categories of events, with one or two jets identified as b jets, are selected. In the final selected samples shown in Fig. 2, the background is approximately a factor of 50 that of the s-channel signal, and a factor of 30 that of the t-channel. Moreover, the uncertainties on the background processes are larger than the expected signal. To measure the production cross section, the expected rate for signal must clearly exceed the uncertainty on the background, which requires additional signal-background separation to obtain a purer sample of signal events.

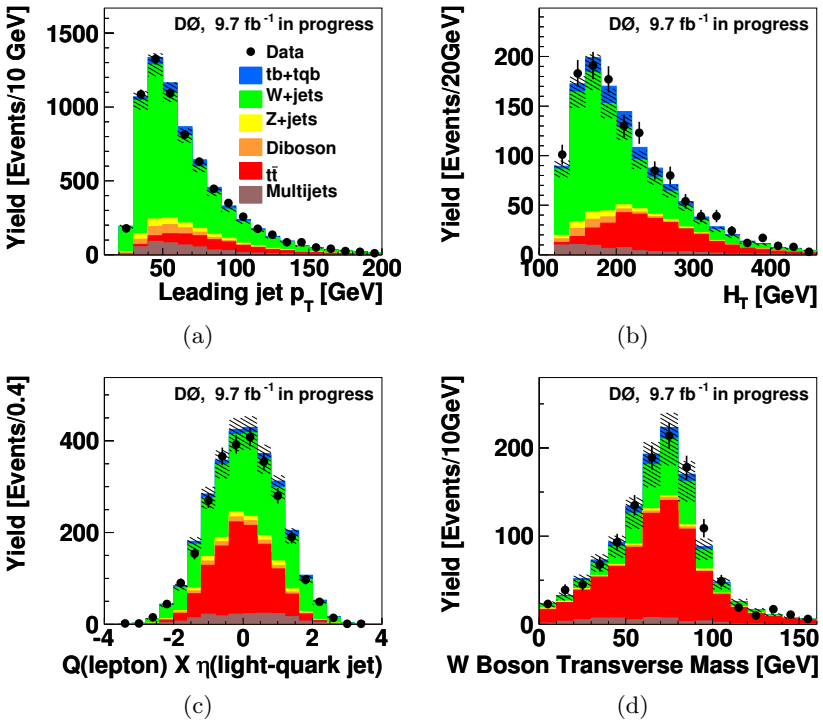

Fig. 2. – Comparisons between data and simulation for (a) leading jet p_{T} in 1b-tag, 2jets channel, (b) H_T in 2b-tags, 2jets channel, (c) light quark jet pseudorapidity multiplied by lepton charge ($Q \times \eta$) in 1b-tag, 3jets channel, and (d) W boson transverse mass in 2b-tags, 3jets channel. The hatched bands show the ± 1 SD uncertainty on the background prediction.

3. – Matrix Element Method

However, kinematic properties of the single top-quark events are not very distinct, and there is not a single kinematic variable that can be used to distinguish the signals from background. To obtain a signal-enriched sample, different multivariate analysis (MVA) techniques have been developed [25, 26], exploiting multiple kinematic properties of the signal.

The Matrix Element (ME) method is used to establish the discriminant in this analysis. For each event, the ME method takes the theoretical prediction from the square of the matrix element, $|\mathcal{M}|^2$, and evaluates a probability that it can be described by any given theoretical process. Because the four-momenta of the specific colliding partons are unknown, $|\mathcal{M}|^2$ is convoluted with the parton density function (PDF) for the incident hadrons, and all possible flavor contributions of colliding partons to the process must be summed. In addition, the difference between the initially produced objects in the hard collision and the reconstructed physical particles arising from hadronization and detector resolution is taken into account through a convolution of $|\mathcal{M}|^2$ with a transfer function, $W(\vec{x}, \vec{y})$ that describes the probability to reconstruct a produced state $\vec{y}$ as the final observed state $\vec{x}$ in the detector. As it is not known which jet originates from which parton, the integration has to be summed over all the possibilities of jet-to-parton assignments. Hence, the probability for observing an event with reconstructed four-momenta, $\vec{x}$, can be written as

$$P(\vec{x}) = \frac{1}{\sigma^{obs}} \sum_{\substack{\text{jet-parton} \\ \text{assignments}}} \sum_{i,j} \int d\xi_1 d\xi_2 f_i(\xi_1) f_j(\xi_2) \frac{d\sigma}{dy}(p_1(i)p_2(j) \to y) W(\vec{x}, \vec{y}) dy, \tag{1}$$

where $\frac{d\sigma}{dy}(p_1(i)p_2(j) \to y)$ is proportional to $|\mathcal{M}|^2$, $f_i(\xi_1)$ denote the probability densities for having a parton of flavor i and momentum fraction ξ_1 in the proton, and $f_j(\xi_2)$ denotes the analogous quantity from the antiproton. σ^{obs} is the total observed cross section in the detector. Throughout the evaluation, all correlations among the final-state particles can be retained.

We include the ME formulations for the signal processes, as well as for the main background processes in our final sample, as listed in Table I. The matrix elements are obtained from the MadGraph leading-order ME generator [27], and the CTEQ6L PDF [28] are used for the initial-state parton density. The transfer functions for electrons, muons, jets, and jets misidentified as electrons are determined from the simulated samples. Also, the outputs of the b-jet identification for each jet are utilized in the calculation of the jet-to-parton assignments.

We use the likelihood ratio to define our discriminant:

$$D(\vec{x}) = \mathcal{L}R(\vec{x}) = \frac{\mathcal{L}(S|\vec{x})}{\mathcal{L}(S|\vec{x}) + \mathcal{L}(B|\vec{x})} \tag{2}$$

where the $\mathcal{L}(S|\vec{x})$ and the $\mathcal{L}(B|\vec{x})$ are, respectively, the signal and the background likelihood functions for each event with reconstructed final state $\vec{x}$. The likelihood function is defined as a sum over the signal or background ME probabilities. In particular, the t-channel processes are categorized as background processes when the s-channel discriminant is calculated, and vice versa. The outputs of the s and t-channel discriminants are shown in Fig. 3.

Two Jets		Three Jets	
Name	Process	Name	Process
s-channel			
tb	$u\bar{d} \to t\bar{b} \to \ell^+\nu_\ell b\bar{b}$	tbg	$u\bar{d} \to t\bar{b}g \to \ell^+\nu_\ell b\bar{b}g$
t-channel			
tq	$ub \to td \to \ell^+\nu_\ell bd$	tqb	$ug \to td\bar{b} \to \ell^+\nu_\ell bd\bar{b}$
	$\bar{d}b \to t\bar{u} \to \ell^+\nu_\ell b\bar{u}$		$\bar{d}g \to t\bar{u}\bar{b} \to \ell^+\nu_\ell b\bar{u}\bar{b}$
		tqg	$ub \to tdg \to \ell^+\nu_\ell bdg$
			$\bar{d}b \to t\bar{u}g \to \ell^+\nu_\ell b\bar{u}g$
Background			
Wbb	$u\bar{d} \to Wb\bar{b} \to \ell^+\nu_\ell b\bar{b}$	$Wbbg$	$u\bar{d} \to Wb\bar{b}g \to \ell^+\nu_\ell b\bar{b}g$
Wcg	$sg \to Wcg \to \ell\bar{\nu}_\ell cg$	$Wugg$	$dg \to Wugg \to \ell\bar{\nu}_\ell ugg$
Wgg	$u\bar{d} \to Wgg \to \ell^+\nu_\ell gg$		
WW	$u\bar{u} \to WW \to \ell\bar{\nu}_\ell c\bar{s}$		
WZ	$u\bar{d} \to WZ \to \ell^+\nu_\ell b\bar{b}$		
ggg	$gg \to ggg$		
$t\bar{t}$	$u\bar{u} \to t\bar{t} \to \ell\bar{\nu}_\ell\bar{b}W^+b$	$t\bar{t}$	$u\bar{u} \to t\bar{t} \to \ell\bar{\nu}_\ell\bar{b}W^+b$

TABLE I. – *The processes considered in this analysis in calculating signal and background ME probabilities, including their charge-conjugate states that contain one charged lepton in the final state.*

4. – Result

The resulting binned distribution of the ME discriminant from the four analysis channels (2 or 3 jets with 1 or 2 b-tags) is used for the cross section measurements. A Bayesian approach [15,26] is utilized to extract the cross section. We assume a Poisson distribution for the number of events in each bin, and an uniform, non-negative prior probability for the signal cross section. A posterior probability density function is thereby constructed, taking into account all statistical, systematic uncertainties, as well as their correlations. The position of the peak of the posterior density is defined as the central value of the cross section, and the 68% interval about the peak is taken as an estimate of its uncertainty.

Systematic uncertainties arise from the theoretical prediction and the detector modeling. Some of the uncertainties affect only the overall scale, but others affect also the ME discriminant outputs bin by bin. The main uncertainties come from the jet-flavor composition in W+jets events (20%), the prediction of the $t\bar{t}$ cross section (9%), the b-tagging efficiency (up to 8.8%), and the jet energy scale and resolution (up to 1.2%).

To validate the cross section measurement with the ME discriminant, we study the performance of the method in ensembles of pseudoexperiments. The pseudoexperiment samples are generated taking into account all the uncertainties and their correlations, and different ensembles are generated with different values of the signal cross sections. The average cross section and the average uncertainty for each ensemble are taken as the "ensemble average result." From the results shown in Fig. 4, we conclude that the bias in the ME method is negligible, and we therefore do not calibrate the cross section measurements.

We use the ensemble average results from the ensembles with the SM signal predic-

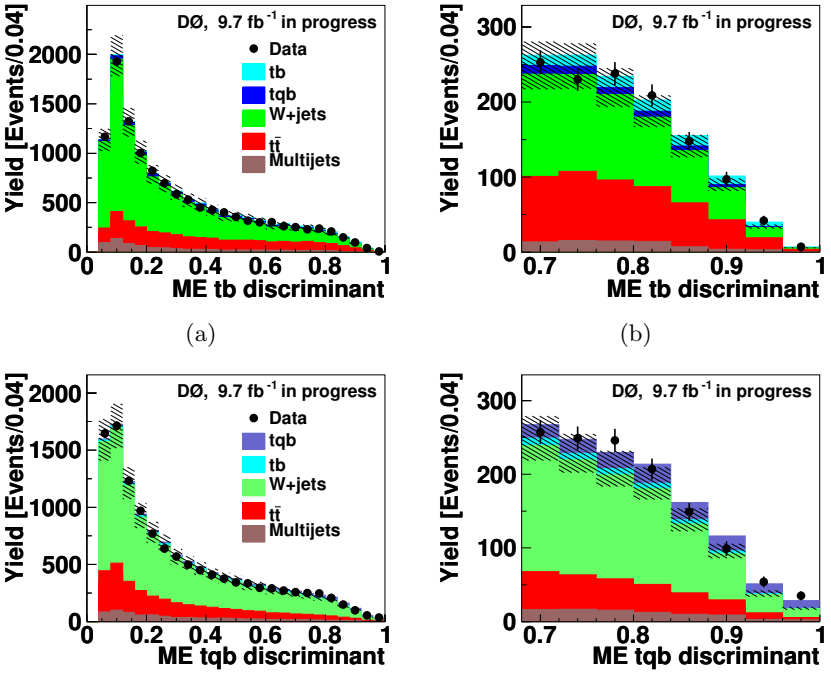

Fig. 3. – Distributions of (a) s-channel and (c) t-channel ME discriminants for the combined analysis channels in the entire region. Distributions of (b) s-channel and (d) t-channel ME discriminants for the combined analysis channels in the signal-enriched region. The hatched bands show the ± 1 SD uncertainty on the background prediction.

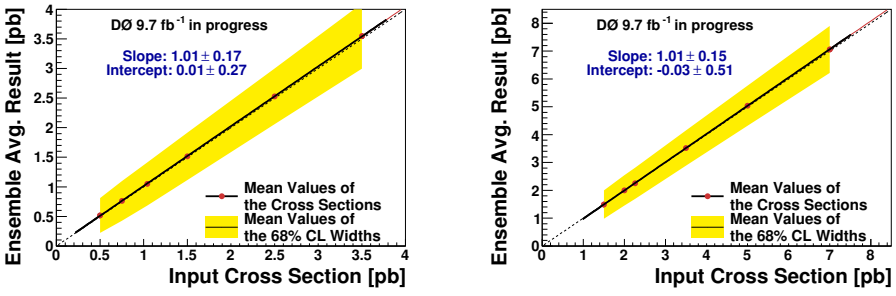

Fig. 4. – The ensemble average results of measured cross sections as a function of the input cross sections for (a) s-channel and (b) t-channel. The band shows the ensemble average of the 68% interval of the posterior density, and this interval is used as the uncertainty of the value of the cross section in the fit.

tions, 1.04 pb and 2.26 pb for the s and t-channels respectively, as the expected results:

$$\sigma^{\rm exp}(p\bar{p} \to tb + X) = 1.05^{+0.38}_{-0.35} \text{ pb}$$
$$\sigma^{\rm exp}(p\bar{p} \to tqb + X) = 2.26^{+0.58}_{-0.54} \text{ pb}.$$

We assume the SM t-channel when extracting the s-channel cross section, and vice versa.

The significance is quantified by a p-value, which in our case represents how likely the data could statistically fluctuate up to be equal to or greater than the measured value, assuming the signal process is absent. We use the asymptotic log-likelihood ratio approach [29] to evaluate the p-values, which are expected to be 5.5×10^{-4} for the s-channel and 5.8×10^{-7} for the t-channel, corresponding, respectively, to 3.3 and 4.9 standard deviation significance.

5. – Conclusion

In conclusion, we measure the s and t-channel single top-quark production cross sections based on the full Tevatron Run II data collected at the DØ detector, corresponding to 9.7 fb^{-1} of integrated luminosity. The results based on the Matrix Element method are expected to be $\sigma(p\bar{p} \to tb + X) = 1.05^{+0.38}_{-0.35}$ pb and $\sigma(p\bar{p} \to tqb + X) = 2.26^{+0.58}_{-0.54}$ pb. This measurement will be a legacy measurement at the proton-antiproton collider at a center-of-mass of 1.96 TeV. We will combine these results and the other two multivariate analyses, Boosted Decision Tree (BDT) and Neural Network (NN), and will have the results with data soon.

* * *

We thank the staffs at Fermilab and the collaborating institutes.

REFERENCES

[1] Moch S. and Uwer P., *Phys. Rev. D*, **78** (2008) 034003. At $m_t = 172.5$ GeV, $\sigma(p\bar{p} \to t\bar{t} + X) = 7.46$ pb.
[2] Kidonakis N., *Phys. Rev. D*, **74** (2006) 114012. The cross sections for the single top quark processes ($m_t = 172.5$ GeV) are 1.04 ± 0.04 pb (s channel), 2.26 ± 0.12 pb (t channel), and 0.28 ± 0.06 pb (tW channel).
[3] Cortese S. and Petronzio R., *Phys. Lett. B*, **253** (1991) 494.
[4] Willenbrock S. S. D. and Dicus D. A., *Phys. Rev. D*, **34** (1986) 155.
[5] Yuan C.-P., *Phys. Rev. D*, **41** (1990) 42.
[6] Cabibbo N., *Phys. Rev. Lett.*, **10** (1963) 531;
Kobayashi M. and Maskawa T., *Prog. Theor. Phys.*, **49** (1973) 652.
[7] Jikia G. V. and Slabospitsky S. R., *Phys. Lett. B*, **295** (1992) 136.
[8] Abazov V. M. et al. (DØ Collaboration), *Phys. Rev. Lett.*, **106** (2011) 022001;
Abazov V. M. et al. (DØ Collaboration), *Phys. Rev. D*, **85** (2012) 091104.
[9] Tait T. and Yuan C.-P., *Phys. Rev. D*, **63** (2001) 014018.
[10] Abazov V. M. et al. (DØ Collaboration), *Phys. Rev. Lett.*, **102** (2009) 191802.
[11] Abazov V. M. et al. (DØ Collaboration), *Phys. Lett. B*, **641** (2006) 423; *Phys. Rev. Lett.*, **100** (2008) 211803; *Phys. Lett. B*, **699** (2011) 145.
[12] Heinson A. P., Belyaev A. S. and Boos E. E., *Phys. Rev. D*, **56** (1997) 3114.

[13] Abazov V. M. et al. (DØ Collaboration), *Phys. Rev. Lett.*, **101** (2008) 221801; *Phys. Rev. Lett.*, **102** (2009) 092002; *Phys. Lett. B*, **708** (2012) 21.
[14] Abazov V. M. et al. (DØ Collaboration), *Phys. Rev. Lett.*, **99** (2007) 191802; *Phys. Lett. B*, **693** (2010) 81.
[15] Abazov V. M. et al. (DØ Collaboration), *Phys. Rev. Lett.*, **103** (2009) 092001.
[16] Aaltonen T. et al. (CDF Collaboration), *Phys. Rev. Lett.*, **103** (2009) 092002.
[17] Abe F. et al. (CDF Collaboration), *Phys. Rev. Lett.*, **74** (1995) 2626.
[18] Abachi S. et al. (DØ Collaboration), *Phys. Rev. Lett.*, **74** (1995) 2632.
[19] Boos E. E. et al., *Phys. Atom. Nucl.*, **69** (2006) 1317. We use singletop version 4.2p1.
[20] Mangano M. L. et al., *J. High Energy Phys.*, **07** (2003) 001. We use alpgen version 2.11.
[21] Sjöstrand T., Mrenna S., and Skands P., *J. High Energy Phys.*, **05** (2006) 026. We use pythia version 6.409.
[22] Brun R. and Carminati F., *CERN Program Library Long Writeup, Report No. W5013 1993*, **.** (
)
[23] Abazov V. M. et al. (DØ Collaboration), *Nucl. Instrum. Methods in Phys. Res. Sect. A*, **565** (2006) 463; *Nucl. Instrum. Methods in Phys. Res. Sect. A*, **584** (2008) 75; *Nucl. Instrum. Methods in Phys. Res. Sect. A*, **622** (2010) 298.
[24] Abazov V. M. et al. (DØ Collaboration), *Nucl. Instrum. Methods in Phys. Res. Sect. A*, **620** (2010) 490.
[25] Abazov V. M. et al. (DØ Collaboration), *Phys. Rev. D*, **75** (2007) 092007.
[26] Abazov V. M. et al. (DØ Collaboration), *Phys. Rev. D*, **78** (2008) 012005.
[27] Maltoni F. and Stelzer T., *J. High Energy Phys.*, **2003** (2003) .
[28] Pumplin J., Belyaev A., Huston J., Stump D. and Tung W.-K., *J. High Energy Phys.*, **2006** (2006) .
[29] Cowan G., Cranmer K., Gross E. and Vitells O., *Eur. Phys. J. C*, **71** (2010) .